Office of Naval Research (ONR)

Research Performance Ps Report (RPPR)
Contract N629091712176
VERSATILE ADAPTIVE MICRO TURBOFAN ENGINE DEVELOPMENT FOR UAS APPLICATIONS

1. Accomplishments: Summary

The project scope has been divided into six tasks: Task I is concerned with establishing an analytic engine model, Task II comprises the design of inlet and test cell design for ground testing, Task III is related to the design of a fan suitable for the existing engine core, Task IV relates to the design and integration of a gearbox transmission between fan and engine core and Task V outlines the fabrication and assembly of a versatile engine prototype and Task VI involves the testing and comparison between the prototype and alternative cycles. Until month 28 the project was running according to schedule, from this month and on COVID had begun and many lab activities were halted. Due to this the project was granted a year automatic extension. Currently, the project is in month 44 and the progress in the three tasks can be concluded as follows:

- **Task I:** Analytic engine model fully concluded in year 1 and 2.
- **Task II:** Test cell manufacturing and testing has concluded on schedule.
- **Task III:** Fan design including all simulation and analysis has concluded on time.

- **Task IV:** Design of gearbox was concluded, gearbox is in advanced assembly stage.
- **Task V:** Fabrication of engine components was completed, and is in advanced assembly stage.
- **Task VI:** Assembly of engine components have not been completed, and therefore testing has not begun as of the writing of this report.

In the following, the accomplishments in each task will be specified:

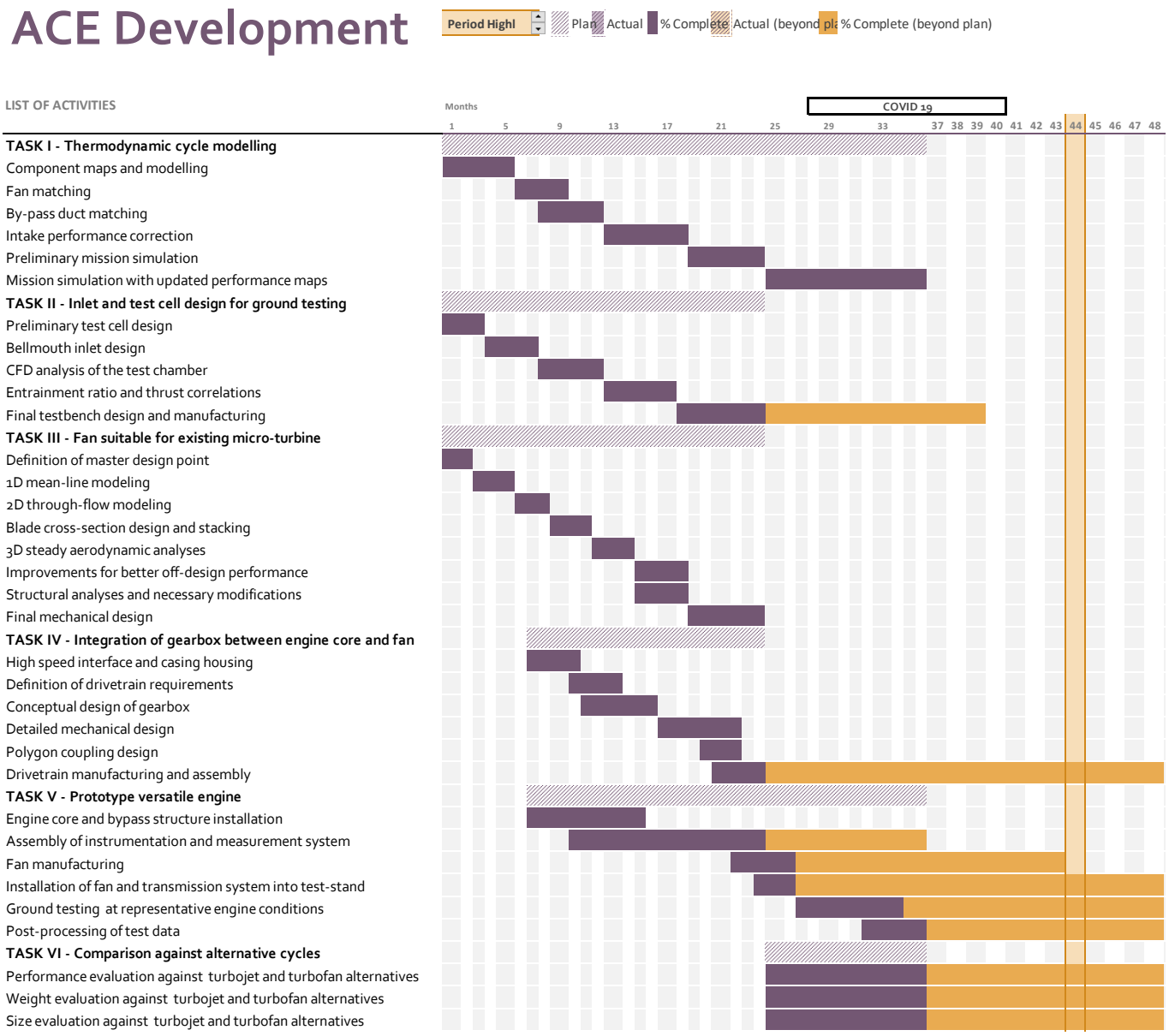

1.1 Thermodynamic cycle modelling

Thermodynamic Cycle Modelling

In order to better define the engine requirements and evaluate the potential benefits associated with the micro-turbojet to micro-turbofan conversion, it is possible to simulate the behavior of the engine in various configurations during a representative flight mission. The simulations are studied using an in-house

MATLAB simulation framework, where AMT "Olympus" component maps, available from open literature, where scaled up and used to simulate the AMT "Nike" engine performance based on declared specification of the manufacturer. At the time of the study, there were no available fan maps in open-literature particular for this scale. Therefore, the fan model from NASA's "Experimental Quiet Engine Program" was selected and modified for the intended application. The core stream map was scaled to meet the mass flow rate requirements of the compressor in its design condition. The bypass map was scaled according to the maximum additional power that can be extracted from the turbine, Figure 1. For the practical limits, pressure ratio for the fan core and bypass stream were selected to be 1.6 and 1.4 respectively.

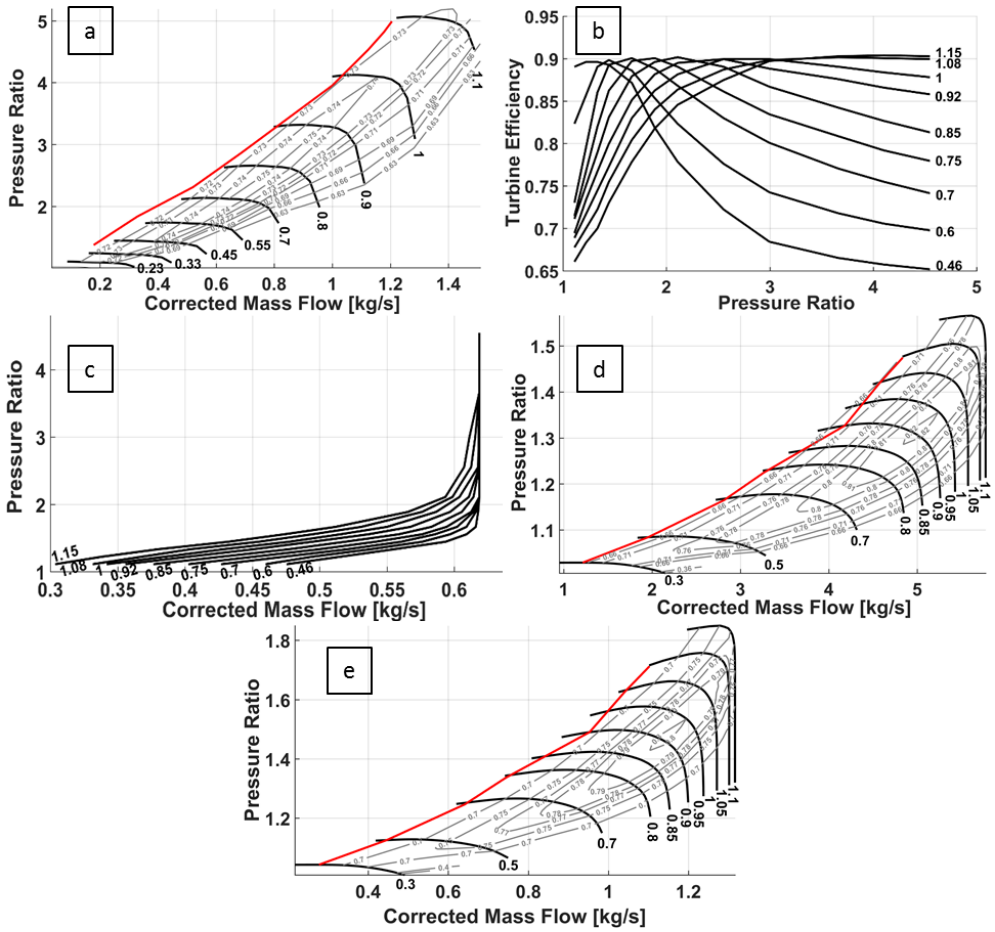

Figure 1: Engine Component Maps. a) Compressor Map; b) Turbine Efficiency map; c) Turbine Pressure Ratio Map; d) Fan Bypass map; e) Fan Core Map

The analysis were conducted for three major segments of the flight: take-off, cruise and loiter. The simulations performed in order to evaluate the benefits of the adaptive cycle turbofan. Thereby, the baseline turbojet is contrasted against fixed-gear/constant-bypass, fixed-gear/variable-bypass, and variable-gear/variable-bypass (adaptive) turbofans. In the case of adaptive turbofan, the produced thrust and required fuel consumption are calculated for each gear ratio - bypass - RPM combination. The data sets that result in minimal fuel consumption at a given thrust level are selected as the engine operating condition. However, in the case of fixed-gear/variable-bypass engine, only the bypass value can vary as the shaft speed changes. The results are compared in terms of fuel consumption vs. required thrust. The results for loiter condition ($h = 5\ [km], M = 0.3$) are summarized in Figure 2. As expected, conversion of turbojet into fixed-gear/fixed-bypass turbofan (blue and red lines, respectively) effectively doubles the thrust potential of the

engine. If the micro-turbine is then equipped with a variable bypass (yellow line), the bypass ratio can be optimized towards most effective operating condition via bypass flow control, resulting in additional increase in operability (22% in thrust) at reduced fuel consumption by 7%. Finally, when CVT gearbox is introduced into the engine (purple line) and introduces an additional degree of freedom to the system, the fuel consumption is further decreased for similar thrust levels, reaching up to 15% savings at 300N thrust with respect to fixed-gear/variable-bypass turbofan. However, at the condition of maximal thrust, there are no advantages for CVT coupled engine as this constitutes the reference "design" state of the fixed gear configuration, and the two engine architectures perform identically.

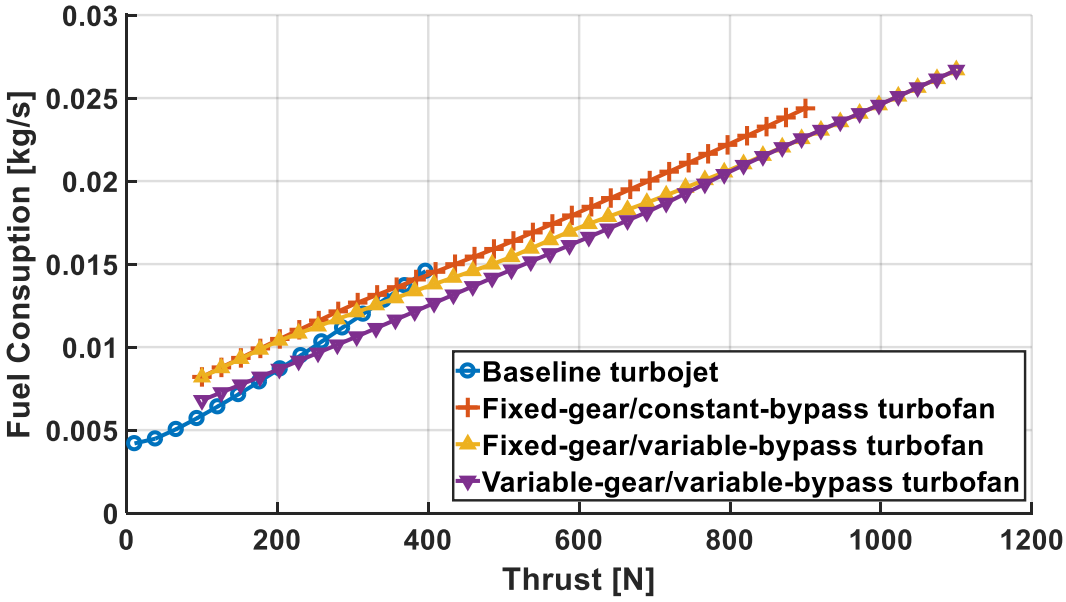

Figure 2: Fuel Consumption vs. Thrust for Various Engine Architecture at Loiter Condition

At take-off condition ($h = 0\ [km], M = 0$), Figure 3 fixed-gear/fixed-bypass turbofan is capable of increasing thrust by 87% to 1250N when compared to the turbojet. In contrast, addition of the variable bypass increases the operability of the fan, and therefore the fixed-gear/variable-bypass turbofan still maintains higher thrust range (1700N) at lowered fuel consumption by up to 11.3%. In this case, the addition of the variable gear further reduces the fuel consumption up to 15% for thrust output of 700N.

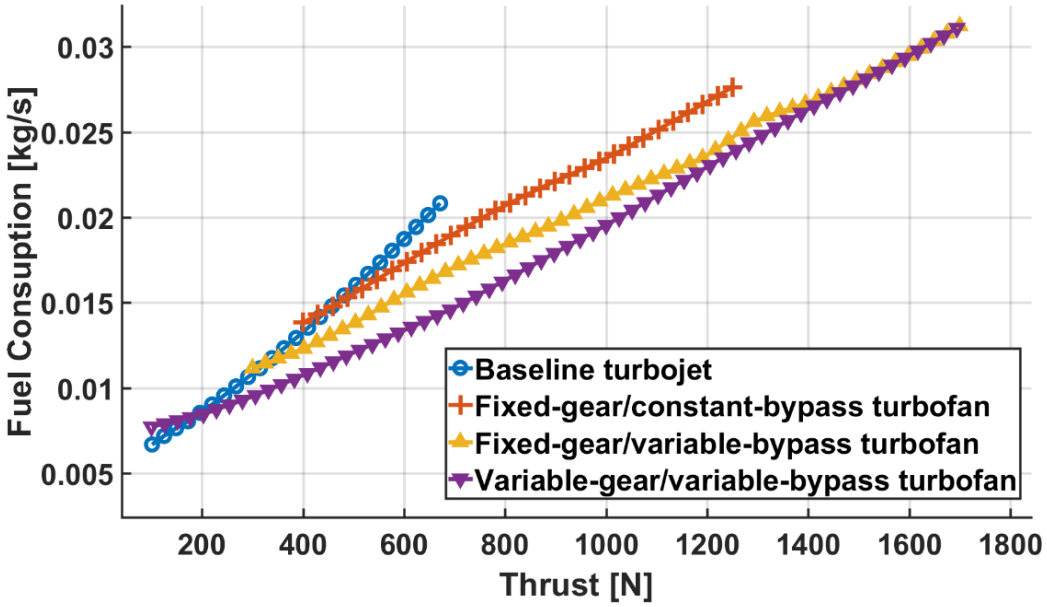

Figure 3: Fuel Consumption vs. Thrust for Various Engine Architectures at take-off Condition

Finally, at cruise condition ($h = 9\,[km], M = 0.9$) Figure 4 can be observed similar trends. Conversion from turbojet to fixed-gear/fixed-bypass turbofan increases maximum thrust by 85%. Addition of the variable bypass yields 8% rise in thrust at improved fuel consumption. Finally, coupling of the CVT further reduces the fuel consumption by up to 7%.

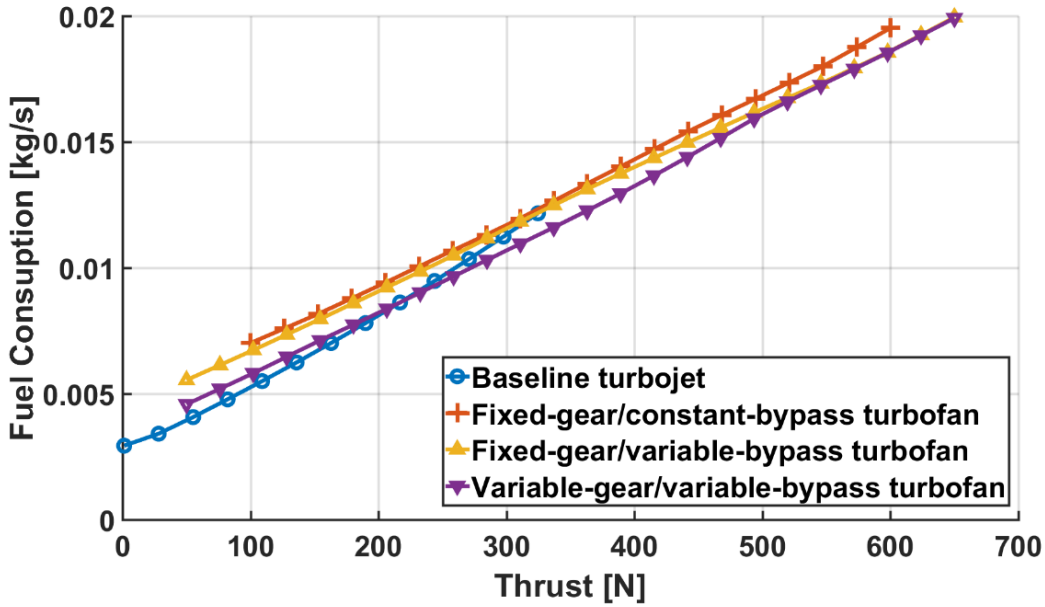

Figure 4: Fuel Consumption vs. Thrust for Various Engine Architectures at Cruise Condition

Transition Algorithm

There are three degrees of freedom in adaptive cycle turbomachine; core speed, variable gear ratio, and bypass nozzle area. Thus, a need for smooth transition between different steady state operating points occur. However, the combinations of these variables for minimal fuel consumptions can result in technically optimal operating lines with sharp transitions. This discontinuity in component level operation is detrimental to overall engine performance and could even lead to complete engine shutdown. Demonstrating the issue, a representative case study focuses on the gear ratio transition between the 1100-1600N thrust levels at take-off conditions, Figure 5. A visible gap is present in gear ratios between 1380N and 1400N, red dots on the transition chart. A more desirable case would be a smooth transition (blue line). However, such arbitrary transitions are not realistic.

Practically, the maximum allowed step can be limited within the simulation. The question is which initial thrust level and its locally optimal variable set should be selected as the starting point for a gradient induced transition limiter. However, this action does not define an optimal path which yields minimum aggregate fuel consumption.

In order to alleviate this problem, the system behavior over the entire operation range should be optimized in the presence of transition constraints. This approach includes construction of a surface consisting of all allowable gear ratio transition lines, each considering a different reference thrust level for the initiation of its gradient-constrained change in variables. Therefore, each line has the optimal variable set for minimum fuel consumption only under its particular thrust level, defined as optimization parameter (Γ). The surface is created through accumulation of all such transitions, Figure 6. Absent of any operational transition constraints, ideal path would consist of traversing the diagonal line in chart (presented by red line in Figure 5). In order to find a global optimum in the presence of transition constraints, the "shortest path" method is implemented to find the most efficient, yet smooth operating line of the engine. Optimized smoothed transition marked by green lines can be seen in figures, Figure 5, Figure 6.

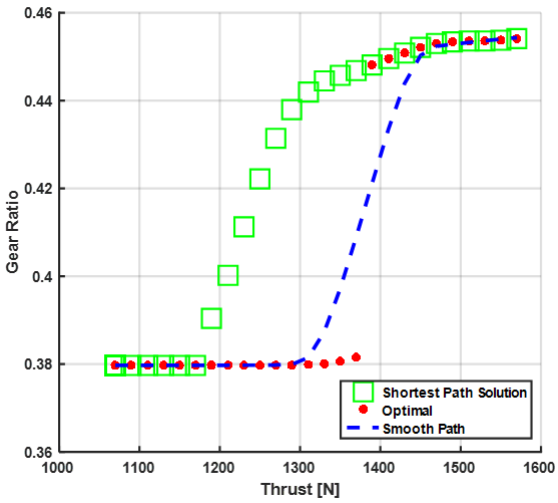

Figure 5: Gear Ratio Transition for 1100-1600N Thrust

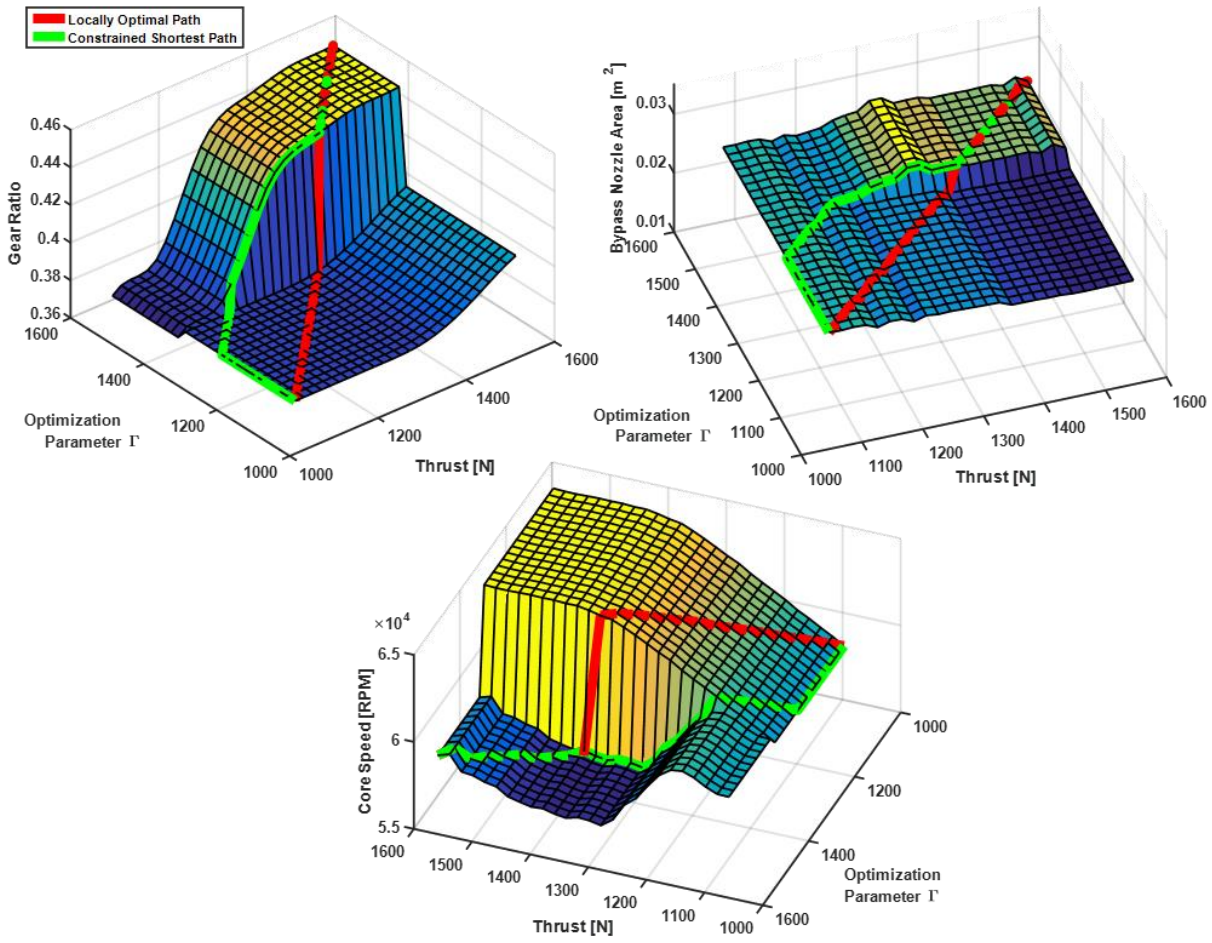

Figure 6: Gear Ratio, Nozzle Area, and Core Speed Transition Optimization for Operation Range

Mission Analysis

To evaluate the necessary aerodynamic properties required for the mission analysis, preliminary design of a representative flying platform was carried out. The main challenge is selection of an aerial vehicle that is relevant in a wide gamut of scenarios. Although most modern UAVs have glider-like shapes and are designed for maximal endurance at slow speeds, Northrop Grumman's X-47B UAV is capable of both fast subsonic flight and slow loiter. Therefore, its shape is considered as the baseline geometry, with twin engine configuration in order to increase the operational range. Proposed layout of such scaled UAV is depicted in Figure 7. The required design properties are summarized in Table 1.

UAVs are widely used around the globe during variety of natural disasters. As they become essential assistants that provide relief services in catastrophic events, it would be of particular interest to contrast the performance of platforms that include fixed-gear/variable-bypass and variable-gear/variable-bypass turbofan configurations as their propulsion systems. Two distinct scenarios are explored: (i) Surveillance and monitoring; and (ii) Active firefighting.

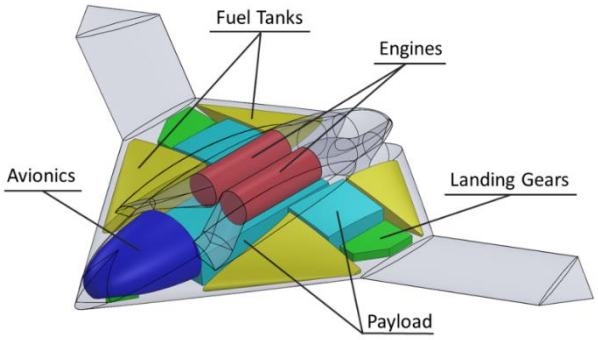

Figure 7: UAV Platform Layout

	$W_0\ [kg]$		$W_e\ [kg]$
Weights	955		477
	C_{D_0}	K	e
Aerodynamics	0.0066	0.103	0.77
	$Length\ [m]$	$Wing\ Span\ [m]$	$S_{ref}\ [m^2]$
Dimensions	3.45	5.5	7.52

Table 1: UAV Design Properties

For the analysis of the surveillance mission, a 1000km remote location is considered to suffer from a natural disaster. At first, the UAV ascends to an altitude of 9km at constant Mach of 0.5. Then, it cruises towards target destination at Mach 0.9. As it approaches its objective, the aircraft descends for 30km at constant Mach of 0.5 to an altitude of 5km and starts loitering above the disaster site with a 5 km turn radius. Then, when the fuel reaches the no-return threshold, the platform follows a similar route to the airfield for refueling. During the last 20km, it will slow down to Mach number 0.3 for safe landing. In order to maximize loiter time, the payload bays are replaced with additional fuel tanks. The goal of the mission is to stay on target for as long as possible. For this mission, the thrust profiles and fuel consumption are charted for both engine types powering the same UAV platform, Figure 8, Figure 9. As the fuel consumption for CVT coupled engine configuration is lower at comparable thrust, the UAV with only variable bypass turbofan engine is forced to return to base earlier due to fuel depletion. The UAV powered by variable-gear/variable-bypass turbofan is able to stay 60 minutes more above the target location, resulting in 20% additional loiter time.

Designed as a multipurpose platform, such a UAV can also serve as crucial aid in putting out forest wildfires, as the vehicle's payload bays are capable of holding up to 365 kg of water. Bush and forest fires became a significant issue during recent years and in order to successfully respond to this phenomenon there is an urgent need to react to even the smallest ignition epicenter. In remote areas, only aviation can

handle this task, but sending large, heavy water-tankers to put out small fires isn't a cost-effective policy. Moreover, due to safety regulations, manned aircrafts are limited to operations during daylight and the resulting night-break can nullify the firefighting efforts. Therefore, cheap, small-size UAVs, present a viable solution to the problem.

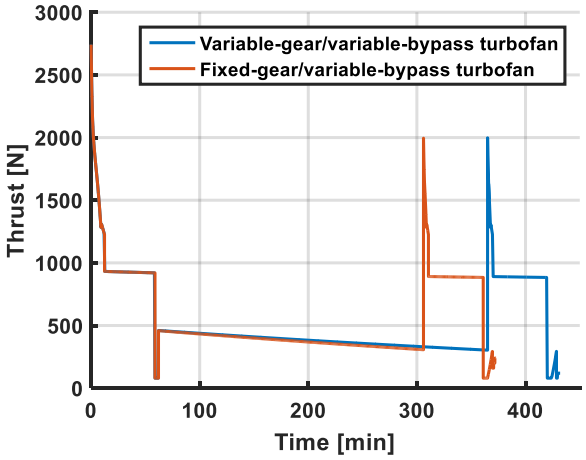

Figure 8: Thrust Profile for Surveillance Mission with Fixed-Gear/Variable-Bypass and Variable-Gear/Variable-Bypass Turbofans

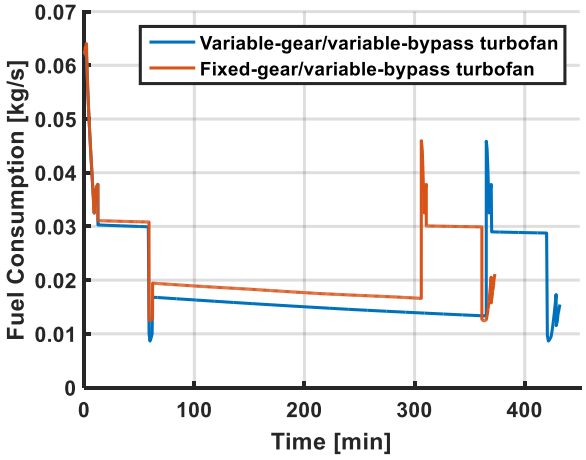

Figure 9: Fuel Consumption profile for Surveillance Mission with Fixed-Gear/Variable-Bypass and Variable-Gear/Variable-Bypass Turbofans

Consider a hypothetical firefighting mission, lasting for six hours of darkness, 300km away from nearest airfield. Such scenario could involve both a leading surveillance UAV and a fleet of three mule firefighters. The leading surveillance UAV ascends to 5km altitude at Mach 0.5 and cruises towards the fire region. Then, it loiters above the location for six hours providing relevant information and guiding the firefighting fleet. At the end of the mission, it returns back to the airfield at constant velocity, descending fort the last 30 km. The firefighter UAVs ascend to 3km altitude and proceed to mission location at constant Mach of 0.5. Then, they slow down to Mach 0.3 and descend the last 30 km to 1km altitude before dropping

their water payload. Finally, they return to base in order to refuel and resupply. As it takes the firefighter UAV about half an hour to reach the burning target, each UAV can complete six full rounds during the mission duration. In the meantime, the surveillance UAV remains above the target the entire duration. The goal of this analysis is to measure the total amount of fuel consumed during the mission. Thrust profile for the entire mission and its fuel consumption are represented in Figure 10 and Figure 11 respectively. The charts show clear advantage of the variable-gear/variable-bypass micro turbofan engines, as the total fuel consumption by the fleet reduces by 12.2% for the entire mission, for an overall fuel saving of 268kg.

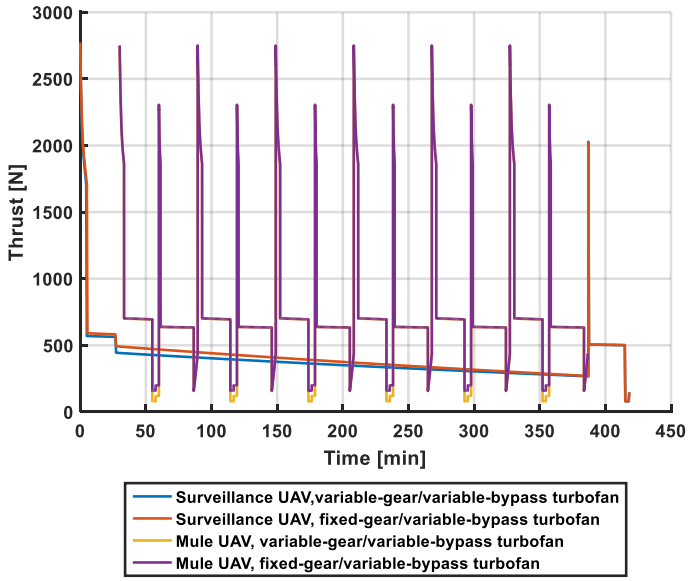

Figure 10: Fuel Consumption profile for Surveillance Mission

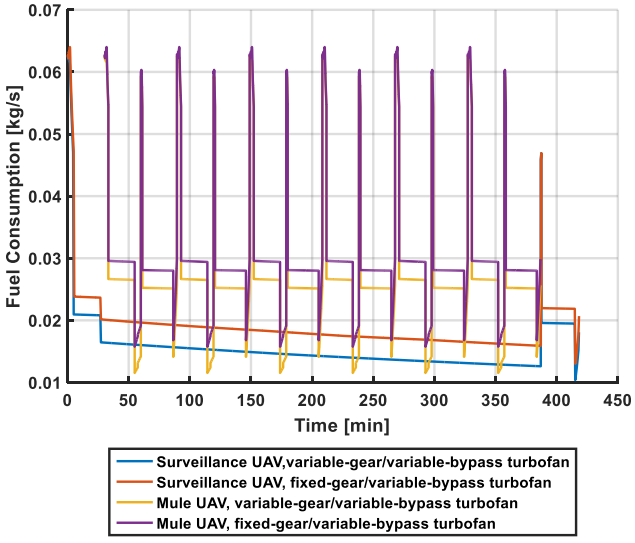

Figure 11: Fuel Consumption Profiles for Firefighting Mission

1.2 Inlet and Test cell design – continued from year 2

In the scope of the ACE engine development, the task of designing a precise and versatile engine thrust test stand, which will be able to accommodate engines of different sizes, is crucial in order to complete the development process. Conservative approach to micro jet engine test stand design usually involves a cradle which supports the engine and slides on plain bearings (Figure 12) or thin plaques that hold the engine in the air and act like springs. In these cases, the thrust measurement device, such as a load cell, is located under or above the engine symmetry axis. Therefore, when using these engine support techniques, the thrust measurement is affected by the friction forces produced in the bearings and the by moments caused due to misalignment between the load cell and the engine axis. In addition to inherently inaccurate measurements, the additional loads and moments in the test stand, vastly contribute to hysteresis phenomenon - dependence of the system state on its history. Within the framework of the present effort, hysteresis is defined as the difference in thrust reading between engine run-up and run-down. Therefore, the main goal of engine test stand development was to minimize the hysteresis and majority of the design efforts were focused on reducing friction and misalignment.

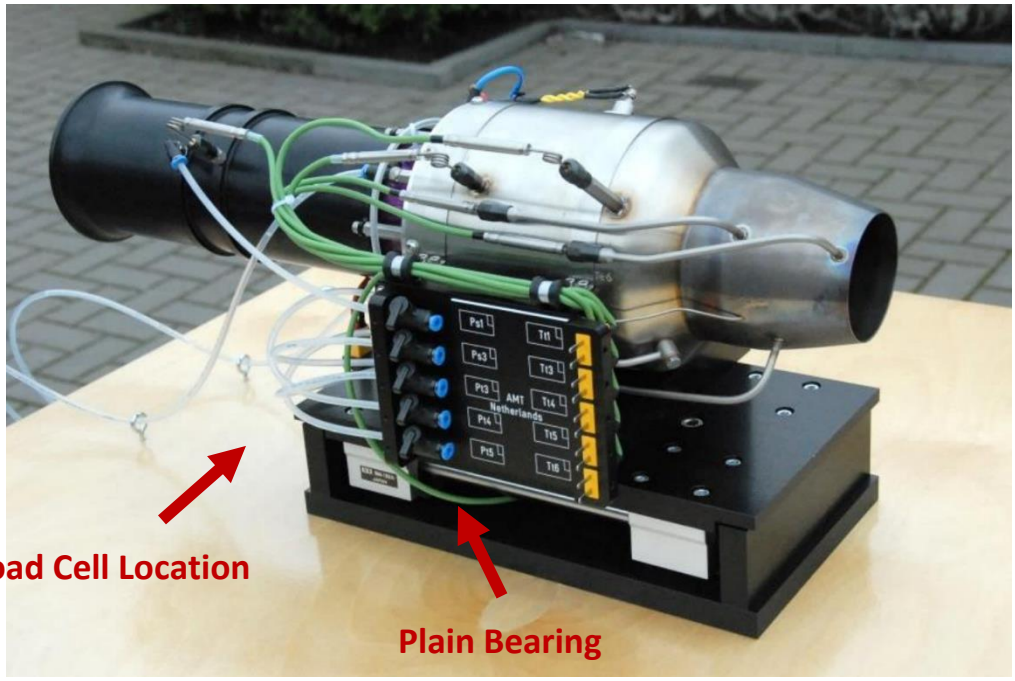

Figure 12: AMT Netherlands engine thrust stand

In an attempt to resolve these challenges, several key approaches are implemented in the test cell design. In order to eliminate potential misalignment effects, the load cell is constrained coaxially to the engine axis. Considering the issue of friction, although the friction losses can't be eliminated completely, they can be minimized. The commonly used plain bearing is the simplest type of bearing, comprising of polished surface and no rolling elements. Therefore, as the journal slides over the bearing surface, it creates a lot of friction. Thus, replacing the bearing system to a more efficient design is the key for overcoming the high friction. Several bearing technologies were reviewed as an alternative while considering their size, load capacity, availability, simplicity and cost. Eventually air bearings technology was selected for the test stand.

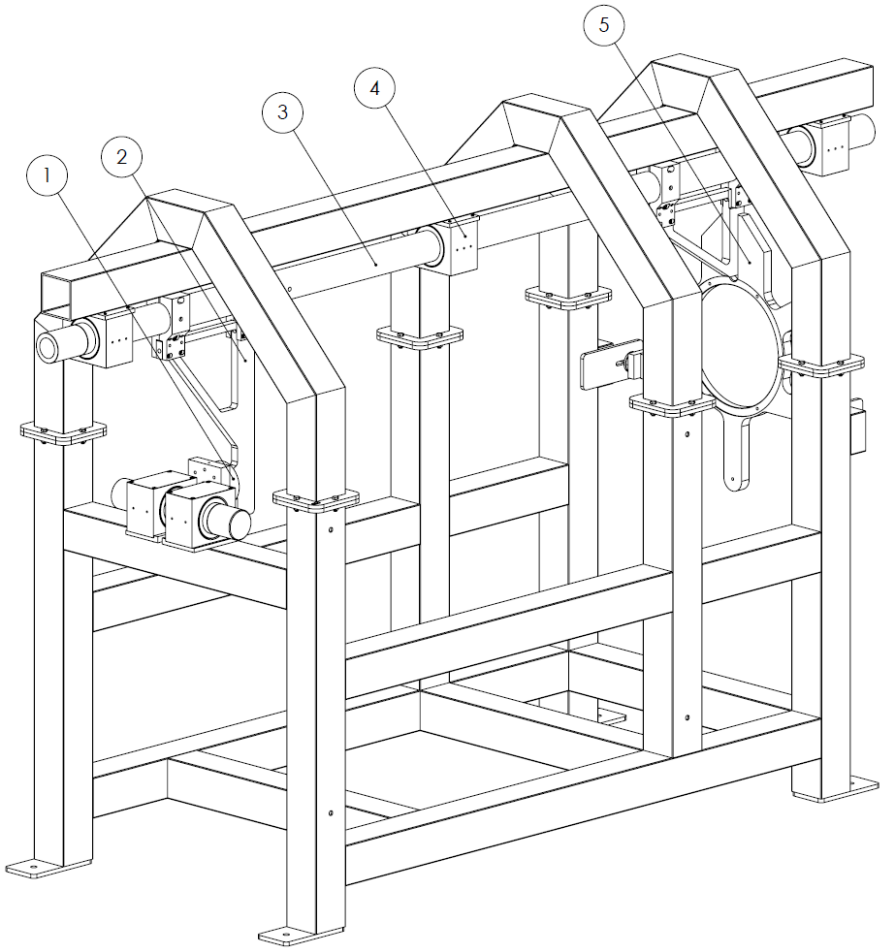

Figure 13: Versatile Engine Test Stand

Figure 13 is describing the basic configuration of the engine test stand final design. Additional components and adapters will be added to accommodate various tested engine models. The test stand structure is built from two pieces and is equipped with five air bearings (4) mounted on precisely machined surfaces. A 75mm shaft (3), which is supported by the bearings, carries the engine mount (5) and the thrust transmitter (2). The engine mount is suitable for any engine with outer diameter of less than 300mm. A dedicated adapter should be designed for every engine and is to be mounted on the engine mount. The thrust of the mounted engine is transferred by the shaft and actuates the load cell (1) via the thrust transmitter. The load cell is rated up to 5kN and can be changed higher loading upon requirement.

As mentioned before, the friction in the system compromises the thrust measurement system accuracy and hysteresis. Although the system friction is dramatically reduced, the measurements are still affected. As a further improvement, quick calibration procedure was developed to be used before every test run. The calibration system is assembled from ten weights of 20kg each, stacked on a metal plate. Electric jack controls the plate height via vertical motion. The weights are connected to calibration adapter, which is attached to the engine during calibration procedure. By lowering the jack height, the weights are pulled up one by one, and thereby, the load cell measures incremental weights in the range of 0-200kg with 20kg steps. The procedure duration takes only a few minutes and in following, the calibration adapter and the weights are removed, allowing for regular engine operation. The experimental data transmitted from the load cell can then be calibrated according to the individual calibration curve of each test.

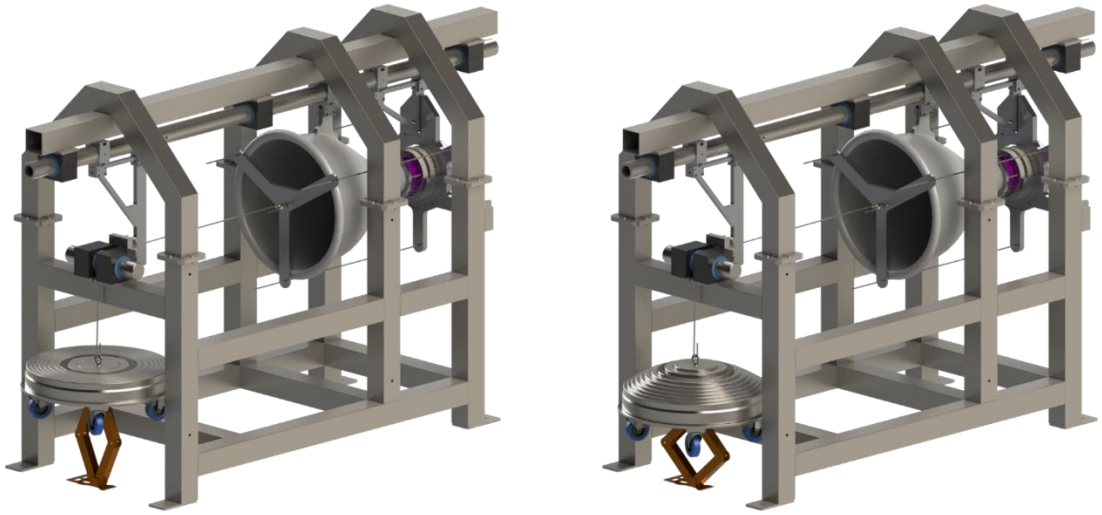

Figure 14: Calibration process: open jack – no load (left), closed jack - 200kg load (right)

1.3 Fan design- continued from year 2

The starting point for the fan design of is the definition of its master design point (MDP), where the fan operation is most critical. As fan's rotational speed is highest in take-off conditions, take-off can be used as fan MDP. The MDP targets are set to:

- Mass flow rate of core: 1.797 kg/sec
- Total pressure ratio of core: 2.0
- Mass flow rate of bypass: 2.178 kg/sec
- Pressure Ratio of bypass: 1.6
- Nominal rotational speed: 33710 RPM

Using previously developed in-house axisymmetric through-flow code, preliminary aerodynamic design is done for the fan stage. The method takes into account each blade section's chord wise loading location in embedded correlations through parabolic camber line assumption. Thus, it becomes mid-loaded double-circular-arc at subsonic and transonic Mach numbers and aft-loaded multiple-circular-arc at supersonic Mach numbers. This methodology enables coupled modeling of bypass and core ducts separated by an aerodynamically shaped flow-splitter as well as the compression stage. Considering stator loss predictions, the peak stage pressure ratio is 2.07 while the minimum pressure ratio is to 1.52. Figure 5 presents the axisymmetric model of the fan design. This approach is described in depth in [4]

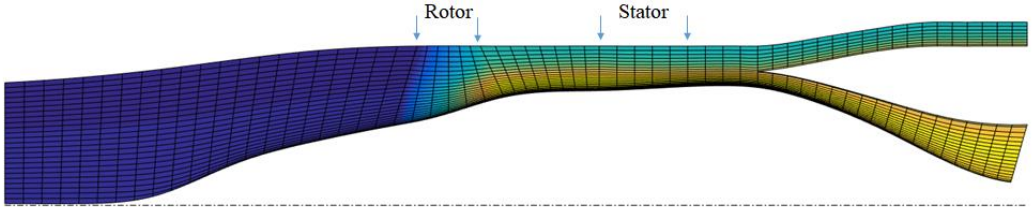

Figure 15: The axisymmetric model of the fan design

ANSYS TurboGrid is then used to create structural turbomachinery computational grids and ANSYS CFX solver is used to compute the steady three-dimensional flow field. Results of the aerodynamic analysis show that due to high hub pressure ratio, the mixing losses in the stator are extremely pronounced. Therefore, the original stator is modified to minimize the stator losses. Initially, split and wide-chord stator is considered, Figure 6. However, the core pressure ratio merely rises to 1.65, which is insufficient according to cycle analysis.

Thus, tandem stator design is tried. In this configuration, if the rear stator is placed near the pressure side of the front stator, it does not block the front suction side and conversely creates a strong suction zone for the neighboring suction side of the front stator [5]. After several iterations of angular shifts and axial

distances, the final geometry is selected to provide stage exit pressure ratio of 1.633 for the outer duct and of 1.796 for the inner duct. However, combined with the diffusion and further mixing, these values drop to 1.574 and 1.725, respectively, at the duct exits.

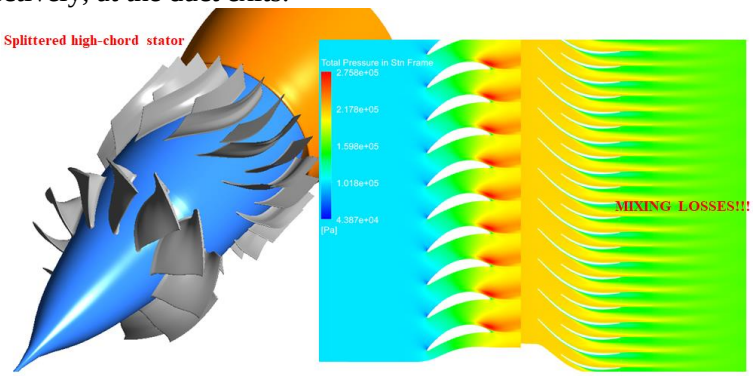

Figure 16: Fan design with split and wide-chord stator, color contours - stationary frame total pressure

As a final check, Figure 7 compares the azimuthal average of total pressure field for the final design with the original stator and the tandem stator. The rotor is only slightly modified between these two designs. It is evident that the tandem stator significantly reduces mixing losses in the inner duct.

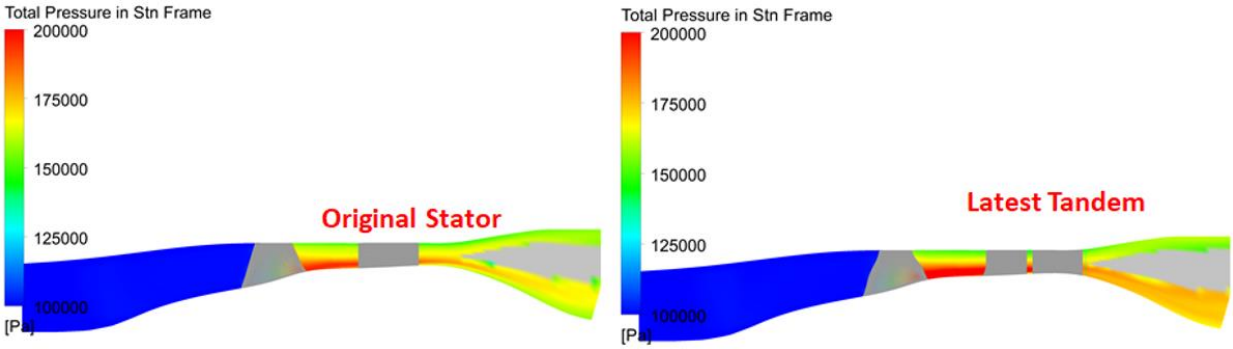

Figure 17: The comparison of azimuthal averaged total pressure for the original stator and the tandem stator

In following, static structural finite element analysis is carried out to observe steady stress levels of the rotor blade. For initial analysis, a bladed disc is designed with a 4mm radius hub fillet identical to the CFD simulations. This blisk can later be optimized to reduce weight. The analyses are carried out in nominal speed and the results are presented in Figure 18. The maximum stress is 350 MPa at the blade root for the nominal speed condition. The safety factor of the blade is 2.6

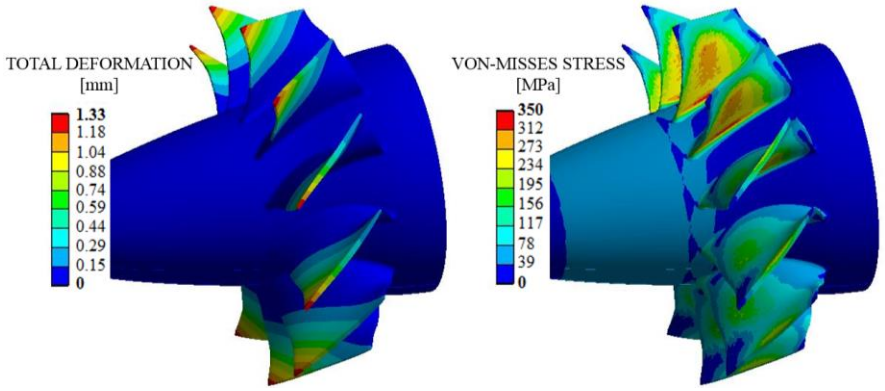

Figure 18: Total deformation and maximal equivalent Von-misses stress at design speed

Rotordynamic analysis is then carried out to find the natural frequencies of the structure. The resonance points are determined via Campbell Diagram for 12th engine order (12 stators),Figure 19. The observed modes are first bending and first torsion modes. These resonance points are around 18000 and 32000 RPM, respectively.

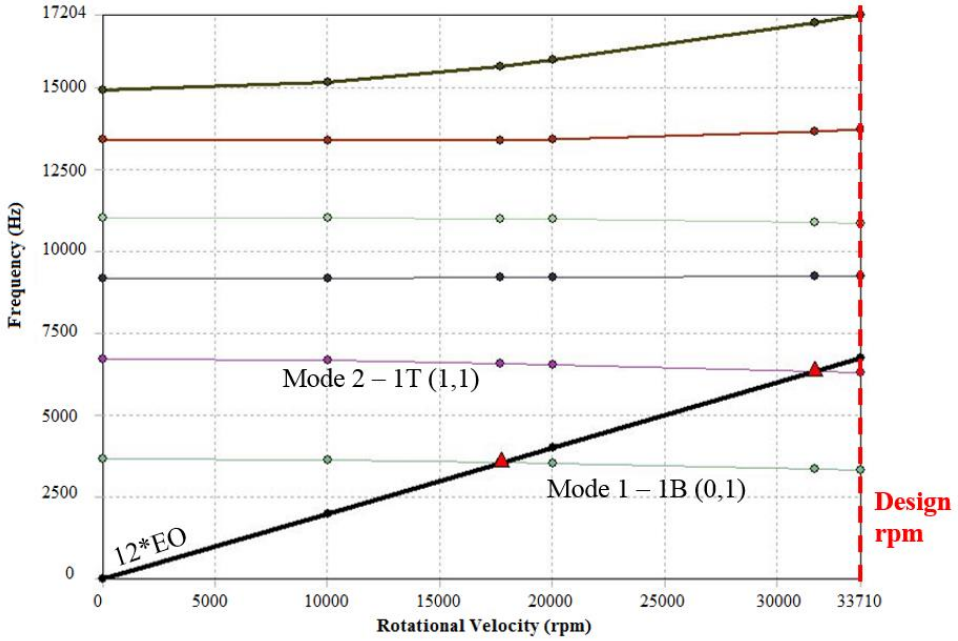

Figure 19: Campbell Diagram of the fan rotor

1.4 Gearbox design and manufacturing

1. Gearbox theoretical analysis

Ideally, the fan is coupled to the turbojet core via continuously variable transmission. Continuously variable transmission will provide a real time, in flight optimization of the fan rotational speed according to changing flight conditions (decoupling the fan speed from the core). This concept is derived from a conventional planetary gearbox, which can already be found in modern turbofan engines where it is widespread due to its compact size, efficient inline speed reduction, high gear ratios and high-power density via division of power among several planet gears. Planetary gearboxes operate by coupling the input and output shafts through a set of coaxial sun and carrier gears, connected by power-transferring planet gears. By adding an alternator or motor as a secondary external speed control input, conventional design can be converted into

continuously variable drivetrain. The variable change in gear ratio is achieved by powering the sun shaft and changing the relative speed between the planets carrier and the ring. Planetary gearbox is a well-known technology and has no limitation on speed or torque transmission. Along with compact design, it makes perfect candidate for currently investigated application.

Usually, the power input is supplied from the sun shaft. Driven part is connected to the carrier. It allows to connect alternator/motor to the ring. However, the load or driving shaft could potentially be attached to either of the rotating components. As a matter of the fact, there are twelve different possible layouts for the planetary gearbox. In the turbofan engine, there is only one source of the power - core of the engine. Fan of the engine performs as power consumer. Short preliminary study was conducted in order to determine which layout of the gearbox would satisfy limitations of the currently investigated adaptive cycle engine. Sign conventions used for the study are explained in Figure 20.

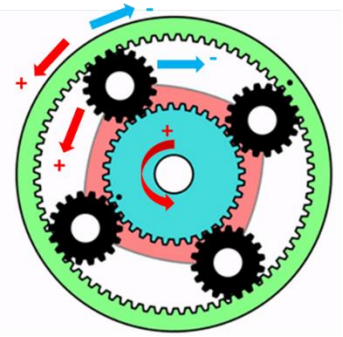

Figure 20: Gearbox sign convention

Speed equations can be derived based on non-slip condition between each gear set. Input and output RPM values are always known and speed of the alternator/motor will be product of this equations. For the sun, the equation can be derived as:

$$\omega_s = -\alpha\omega_R + (1+\alpha)\omega_C \quad (1)$$

For the carrier:

$$\omega_C = [1/(1+\alpha)]\omega_S + [\alpha/(1+\alpha)]\omega_R \quad (2)$$

For the ring and planets:

$$\omega_R = [(1+\alpha)/\alpha]\omega_C - [1/\alpha]\omega_S \quad (3)$$

$$\omega_P = [2\alpha/(\alpha-1)]\omega_R + [(1+\alpha)/(1-\alpha)]\omega_C \quad (4)$$

α is a geometrical variable, which is defined as ratio between ring to sun radii.

Gearbox is considered to be in steady state and therefore, the sum of torques in it must be equal to zero. From the jet engine simulation, speed and power of the core and the fan are known. Thus, torques of the driving and driven shafts can be calculated according to:

$$Tq = PW \cdot 60/2\pi N \quad (5)$$

Therefore, last unknown torque will get the value in such a way, that the gearbox will remain at steady state.

The design point of variable gear ratio turbofan was chosen as a case study for this analysis. In this condition, the core of the engine provides 270.5 kW to the gearbox at 56260 RPM. Fan consumes 260.5 kW at 39223 RPM. Additional 5 kW is spared for the alternator. After analysis of all twelve cases, it been found that only case 7 with α value of 2.33 meets all requirements. For this case, the core of the engine is connected to the ring, the fan is connected to the carrier and the alternator to the sun of the gearbox. Power balance study of this case is depicted in Figure 21.

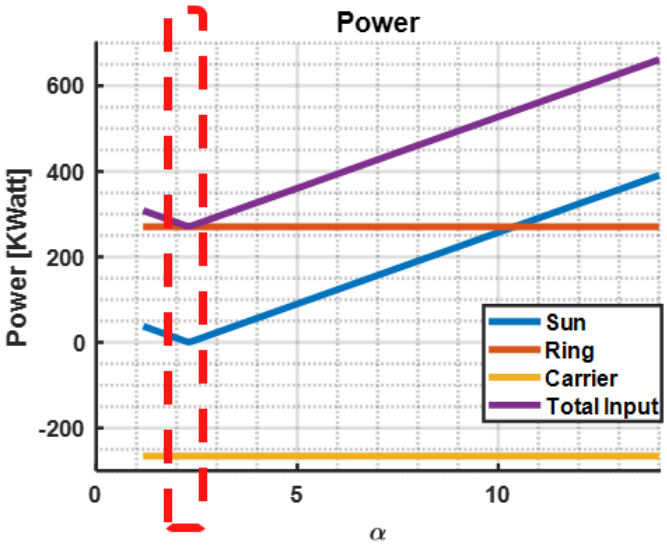

Figure 21: Power balance as function of α for the gearbox

Based on current technological level of redactors and its availability, it was decided to integrate conventional gearbox between engine core and a fan. It also allows to reduce level of complexity and ensures successful completion of the project. Therefore geared turbofan with variable bypass nozzle is considered a sufficient technological step up for the current state of the micro turbojet market.

2. Design and integration

As described in previous paragraph, 1.8 ratio reduction gearbox is considered. Design considerations were - high speed and power transference with small physical dimensions. As described in Figure 22, the proposed gearbox uses a double planetary gear arrangement with a sun gear for each shaft (input (1) and output (2) sides) and a total of 3 planets (9) for each sun which are sitting on the same shaft. This configuration allows to split the power between the planet gears and thus reduce the load on each individual gear. The gearbox also includes threaded holes in the gearbox casing for fan assembly fixing and blind holes for the oil piping (7).

The gearbox also contains two hydrodynamic journal bearing for each planet gear (3), and one for the output gear. Hydrodynamic bearings allow to rotated at very high speeds with relatively low losses. The input gear is supported by two angular contact bearings in “Back-to-Back” configuration (5), which allows a more precise centering between the input shaft and the gearbox casing.

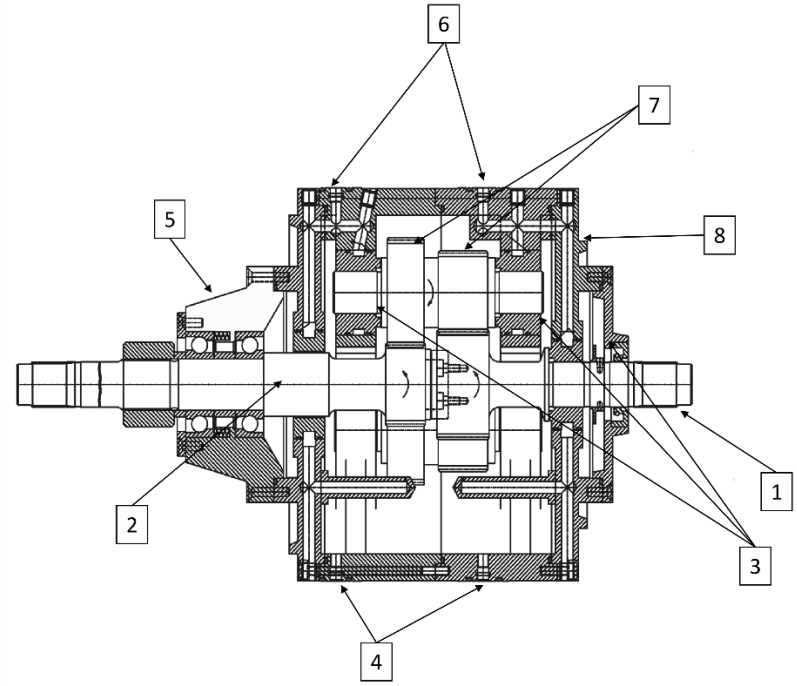

Figure 22: Gearbox cut section and schematic

For proper operation of the gearbox, a lubrication system is needed. This system, which is schematically presented in Figure 23, operates in closed loop and is designed to provide lubrication to the gear meshes, as well as providing constant oil to the hydrodynamic bearings and to evacuate heat that was added to the oil due to shear forces working between the gears and in the bearings. An overview of power losses and oil consumption rates is presented in Table 2.

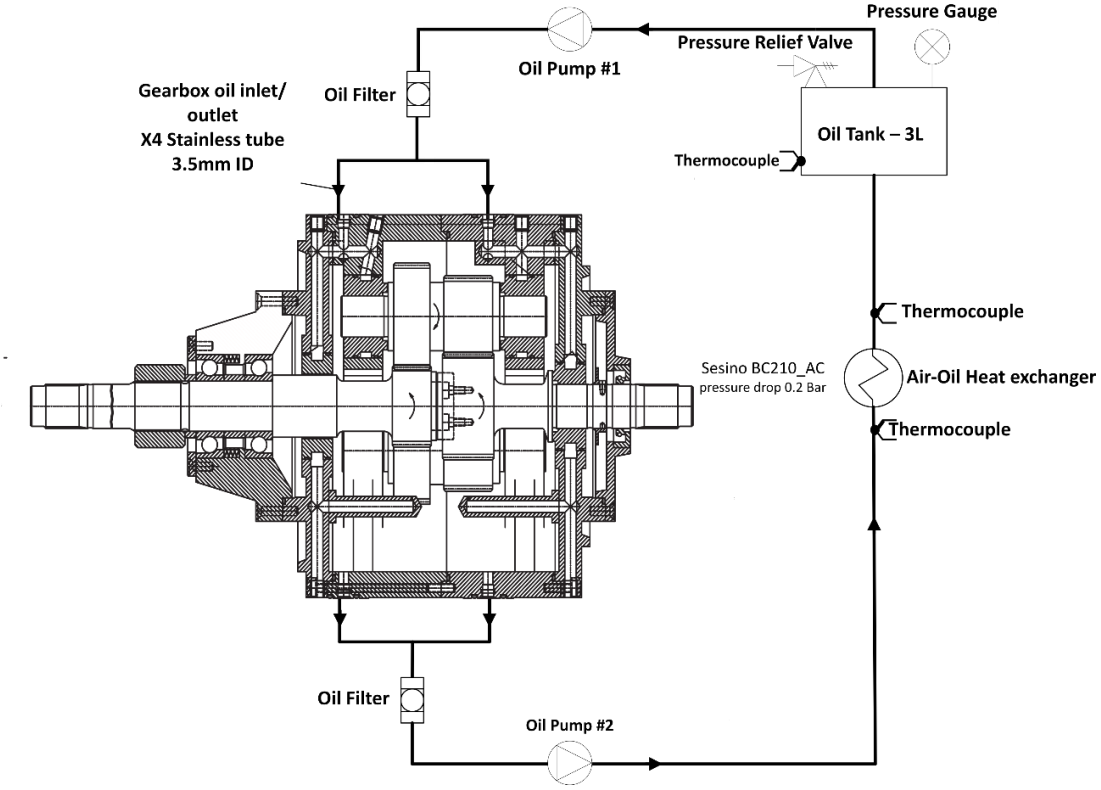

Figure 23: Gearbox lubrication system schematic

Consumer	Quantity	Total power loss [kW]	Total oil flow [l/min]
Gear mesh	6	6x0.34=2.04	6x0.27=1.62
Bearing A	3	3x0.23=0.69	3x0.23=0.69
Bearing B	3	3x0.25=0.75	3x0.24=0.72
Bearing for input shaft	2	2x0.25=0.5 (estimated)	-
Bearing for output shaft	1	0.15	0.12
Total gearbox		4.13	3.15

Table 2: Power losses and oil flow rate in gears and bearings

The basic operation of the system is as following: two volumetric pumps work in tandem at the inlet and outlet of the gearbox, one pushing oil at the inlet Figure 23 (Pump #1) and the other pulling oil at the outlet Figure 23 (Pump #2). These pumps include a priming feature which releases any air trapped in the oil. Inside the gearbox, the oil is sprayed directly on the gears using 3 tooth spray bars, as seen in Figure 24, and is supplied to the bearings using channels in the gearbox casing.

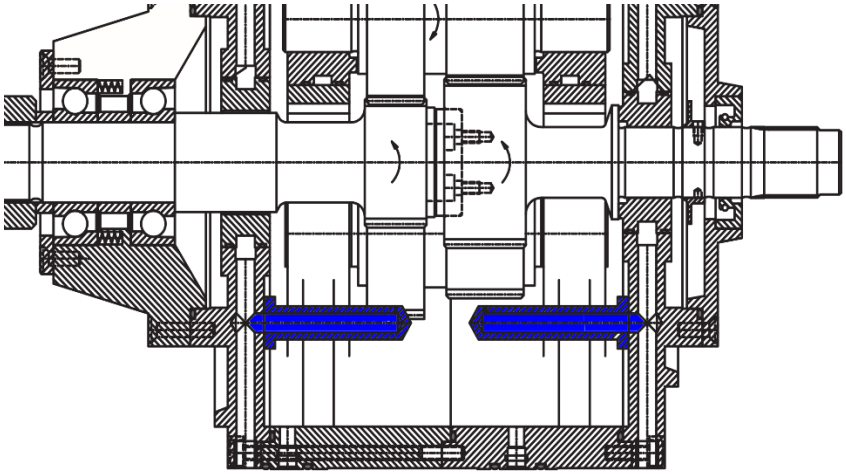

Figure 24: Cut section of gearbox with spray bars (marked in blue)

From the gearbox, the oil flows through an air-to-oil heat-exchanger which works to extract the added heat from the oil and thus reduces its temperature to approximately $60° C$, the oil is then fed into a 3 liter buffer tank and transferred back into the gearbox with Figure 23 (Pump #1).

1.5 Adaptive engine prototype

1.5.1 Engine assembly design:

As the adaptive cycle turbofan is designed around an existing micro gas turbine core, the modifications design, integration and assembly are constrained and necessitate a unique cantilevered design. This architecture is depicted in Figure 25. Thus, the engine consists of 3 main sub-assemblies with all components ultimately supported by the external casing, Figure 26. The variable bypass mechanism is an independent system, which is only attached to the external casing without interfacing with other components. This configuration requires addition of several couplings which transfer torque from the core driving shaft to the fan assembly and from the gearbox output to the fan shaft. External casing is used as a precise reference point towards aligning the different assemblies.

Figure 25: Adaptive cycle engine final assembly design

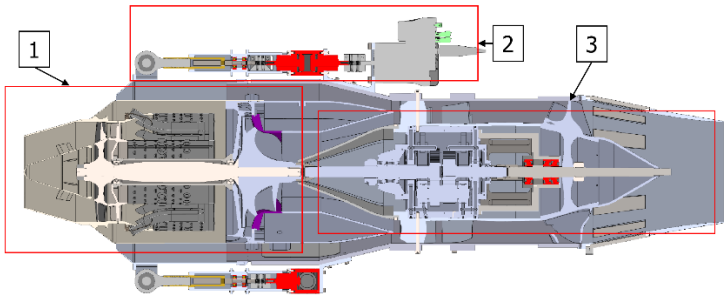

Figure 26: Main engine sub-assemblies - (1) Core, (2) Variable bypass and (3) Fan assembly

In the scope of this report, the manufacturing of all engine components was completed, and the assembly of the engine is advanced stages.

The completely assembled variable bypass mechanism, together with the modified Turbojet core can be seen in Figure 27.

Figure 27: Assembled variable bypass and turbojet core

In Figure 28 the gearbox assembly process is presented.

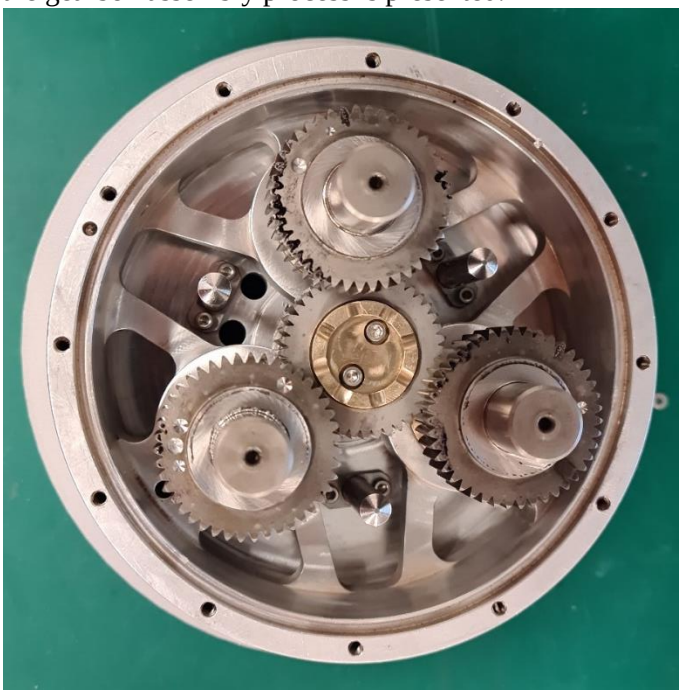

Figure 28: Gearbox assembly

Fan has been manufactured in 2 configurations-

1) Highly twisted configuration which is additively manufactured using SLS printing (Figure 30). This has already been manufactured and is awaiting post-processing (see Figure 29)

Figure 29: Additively Manufactured highly twisted fan

2) CNC manufactured version with less twist. (Figure 30).

Figure 30: CNC manufactured fan

Finally, the fan was assembled together with the external engine casing with the variable bypass mechanism, turbojet core and gearbox as seen in Figure 31.

Figure 31: Assembled turbofan engine (without inlet)

1.5.2 Assembly of instrumentation and measurement system:

Test stand was assembled and tested using the ACE engine core (NIKE). The instrumentation is partially show in Figure 32 and includes:

- Static Pressure:
    1. Bellmouth inlet
    2. Engine Inlet
    3. Ambient
- Static Pressure
    4. Bellmouth Inlet
    5. Ambient
- RPM
- Thrust Load Cell
- Fuel Flow Rate

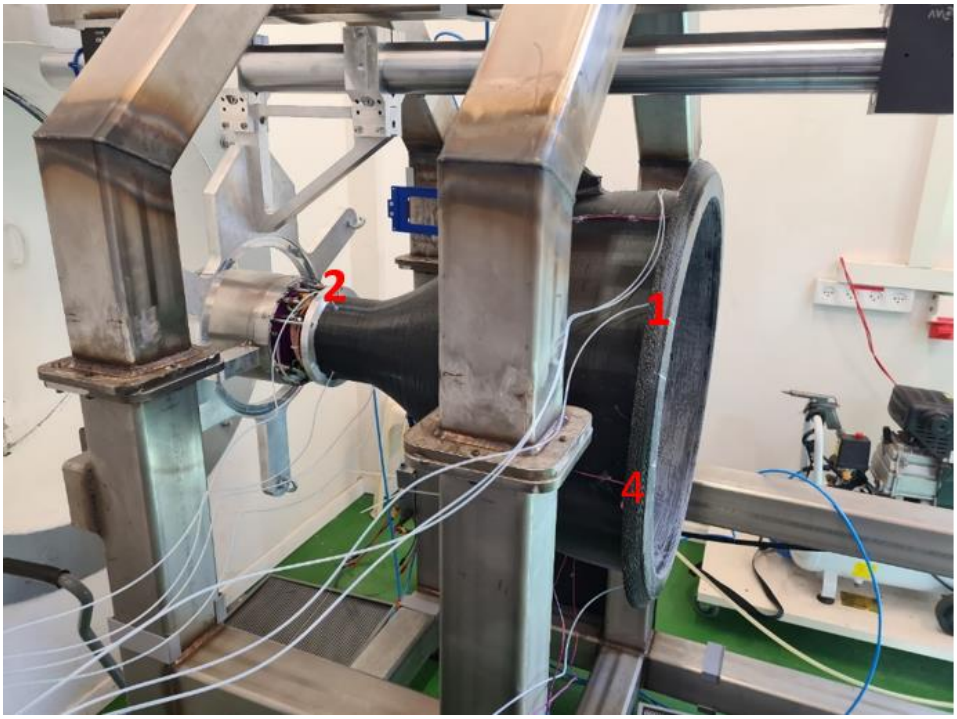

Figure 32: Probe location on test stand

NIKE turbojet core was run and tested using the new test stand and then compared to a CFD simulation run with ANSYS Fluent and additionally compared to an existing test stand made by the engine manufacturer.

Technology Transfer

No

Participants

1. Type: Most senior project role
   Faculty
2. Prefix: Assoc. Prof.
3. First Name: Beni
4. Last Name: Cukurel
5. Nearest person month worked: 28

1. Type:
   Non-Student Research Assistant
2.
3. Prefix: Mr.
4. First Name: David
5. Last Name: Linsky
6. Nearest person month worked: 2

1. Type:
   Non-Student Research Assistant
2. Prefix: Mr.
3. First Name: Ron
4. Last Name: Meizner
5. Nearest person month worked: 15

1. Type:
   Non-Student Research Assistant
2. Prefix: Mr.
3. First Name: Boris
4. Last Name: Leizeronok
5. Nearest person month worked: 22

1. Type:
   Staff Scientist (doctoral level)
2. Prefix: Dr.
3. First Name: Slava
4. Last Name: Losin
5. Nearest person month worked: 2

1. Type:
   Non-Student Research Assistant
2. Prefix: Mr.
3. First Name: Alex
4. Last Name: Kleiman
5. Nearest person month worked: 16

1. Type:
   Non-Student Research Assistant
2. Prefix: Mr.
3. First Name: Michael
4. Last Name: Palman

5. Nearest person month worked: 3

1. Type:

Non-Student Research Assistant

2. Prefix: Mr.
3. First Name: Iliya
4. Last Name: Romm
5. Nearest person month worked: 8

1. Type:

Consultant

2. Prefix: Assoc. Prof.
3. First Name: Sercan
4. Last Name: Acarer
5. Nearest person month worked: 3
6. Country if participant is a foreign collaborator: Turkey

1. Type:

Graduate Student (research assistant)

2. Prefix: Assoc. Mr.
3. First Name: Tayyip
4. Last Name: Gurbuz
5. Nearest person month worked: 23
6. Country if participant is a foreign collaborator: Turkey

Students

- Michael Palman: M.Sc. Student

Products

Below is the information detailed for each product submission:

1. Publications:
    a. Article Title: “Mission Analysis and Operational Optimization of Adaptive Cycle Micro-Turbofan”
    b. Journal: Journal of Engineering for Gas Turbines and Power
    c. Authors: Palman, M., Leizeronok, B., Cukurel, B.
    d. Publication Status: Published
    e. Publication Identifier: 10.1115/1.4040734
    f. Publication Date: September 14, 2018
    g. Volume: Vol. 141
    h. Issue: 1
    i. Publication Location: ASME, New York, NY, US
    j. Acknowledgement of Federal Support? Yes
    k. Peer Reviewed? Yes

    Additional papers are in the final stage in preparation for submission:

    a. Article Title: “Comparative Study of Numerical Approaches to Adaptive Gas Turbine Cycle Analysis”
    b. Journal: International Journal of Turbo and Jet Engines
    c. Authors: Palman, M., Leizeronok, B., Cukurel, B.
    d. Publication Location: De Gruyter, Berlin, Germany
    e. Acknowledgement of Federal Support? Yes

f. . Article Title: “Mechanical Design Considerations in Micro-Turbojet to Adaptive Cycle Micro-Turbofan Conversion”
g. Journal: AIAA Journal of Propulsion and Power
h. Authors: Palman, M., Linsky, D., Meizner, R., Leizeronok, B., Gurbuz, T., Hakyemez, D., Acarer, S., Andreoli, V., Vyas, U., Braun, J., Paniagua, G.
i. Publication Location: Aerospace Research Central (ARC)
j. Acknowledgement of Federal Support? Yes

2. Conference Paper

a. Title: “Mission Analysis and Operational Optimization of Adaptive Cycle Micro-Turbofan”
b. Authors: Palman, M., Leizeronok, B., Cukurel, B.
c. Conference Name: ASME Turbo Expo 2018
d. Conference Date: June 11-15, 2018
e. Conference Location: Oslo, Norway
f. Publication Status: Accepted
g. Publication Date: August 30, 2018
h. Publication Identifier Type: DOI
i. Publication Identifier: 10.1115/GT2018-75323
j. Acknowledgement of Federal Support? Yes

3. Thesis
a. Title: Development of Adaptive Cycle Micro-Turbofan Engine for UAS Applications
b. Institution: Technion Israel Institute of Technology
c. Authors: Michael Palman
d. Completion Date: January 5th, 2020
e. Acknowledgement of Federal Support? No

REPORT DOCUMENTATION PAGE

Form Approved
OMB No. 0704-0188

The public reporting burden for this collection of information is estimated to average 1 hour per response, including the time for reviewing instructions, searching existing data sources, gathering and maintaining the data needed, and completing and reviewing the collection of information. Send comments regarding this burden estimate or any other aspect of this collection of information, including suggestions for reducing the burden, to Department of Defense, Washington Headquarters Services, Directorate for Information Operations and Reports (0704-0188), 1215 Jefferson Davis Highway, Suite 1204, Arlington, VA 22202-4302. Respondents should be aware that notwithstanding any other provision of law, no person shall be subject to any penalty for failing to comply with a collection of information if it does not display a currently valid OMB control number.
PLEASE DO NOT RETURN YOUR FORM TO THE ABOVE ADDRESS.

1. REPORT DATE *(DD-MM-YYYY)*	2. REPORT TYPE	3. DATES COVERED *(From - To)*
	Final	09.29.17-09.28.21

4. TITLE AND SUBTITLE
NICOP - Versatile Adaptive Micro Turbofan Engine Development for UAS Applications

5a. CONTRACT NUMBER

5b. GRANT NUMBER
N62909-17-1-2176

5c. PROGRAM ELEMENT NUMBER

6. AUTHOR(S)
Cukurel, Beni
Linsky, David
Palman, Michael
Acarer, Sercan

5d. PROJECT NUMBER

5e. TASK NUMBER

5f. WORK UNIT NUMBER

7. PERFORMING ORGANIZATION NAME(S) AND ADDRESS(ES)
Technion Research & Development Foundation Ltd.
Technion City
Haifa 3200003 ISRAEL

8. PERFORMING ORGANIZATION REPORT NUMBER
2024486-FINAL

9. SPONSORING/MONITORING AGENCY NAME(S) AND ADDRESS(ES)
Office of Naval Research Global
86 Blenheim Screscent
Ruislip MX HA4 &HB
United Kingdom

10. SPONSOR/MONITOR'S ACRONYM(S)

11. SPONSOR/MONITOR'S REPORT NUMBER(S)

12. DISTRIBUTION/AVAILABILITY STATEMENT
Approved for Public Release; Distribution is Unlimited

13. SUPPLEMENTARY NOTES

14. ABSTRACT
The goal of our project is the development of a variable cycle micro gas turbine engine, which operates via integration of a fan by a fixed gear transmission into an existing micro-turbojet with an adaptive bypass nozzle. The developed solution significantly improves maximum thrust, reduces fuel consumption by maintaining the core independently running at its optimum, and enables a wider operational range, all the meanwhile preserving a simple single spool configuration.

15. SUBJECT TERMS
Turbofan, Turbojet, Adaptive cycle engine, UAV, Aeronautical propulsion, Design optimization, Engines, Intelligent control, Thermodynamics, Aerospace, Propulsion systems, Flight, Gears, Surveillance, Thrust, Unmanned aerial cehicles, Fuel consumption, Cycles

16. SECURITY CLASSIFICATION OF:			17. LIMITATION OF ABSTRACT	18. NUMBER OF PAGES	19a. NAME OF RESPONSIBLE PERSON
a. REPORT	b. ABSTRACT	c. THIS PAGE			Cukurel, Beni
					19b. TELEPHONE NUMBER *(Include area code)*
U	U	U	SAR	27	+972-(0)77-887-1962

INSTRUCTIONS FOR COMPLETING SF 298

1. REPORT DATE. Full publication date, including day, month, if available. Must cite at least the year and be Year 2000 compliant, e.g. 30-06-1998; xx-06-1998; xx-xx-1998.

2. REPORT TYPE. State the type of report, such as final, technical, interim, memorandum, master's thesis, progress, quarterly, research, special, group study, etc.

3. DATE COVERED. Indicate the time during which the work was performed and the report was written, e.g., Jun 1997 - Jun 1998; 1-10 Jun 1996; May - Nov 1998; Nov 1998.

4. TITLE. Enter title and subtitle with volume number and part number, if applicable. On classified documents, enter the title classification in parentheses.

5a. CONTRACT NUMBER. Enter all contract numbers as they appear in the report, e.g. F33315-86-C-5169.

5b. GRANT NUMBER. Enter all grant numbers as they appear in the report. e.g. AFOSR-82-1234.

5c. PROGRAM ELEMENT NUMBER. Enter all program element numbers as they appear in the report, e.g. 61101A.

5e. TASK NUMBER. Enter all task numbers as they appear in the report, e.g. 05; RF0330201; T4112.

5f. WORK UNIT NUMBER. Enter all work unit numbers as they appear in the report, e.g. 001; AFAPL30480105.

6. AUTHOR(S). Enter name(s) of person(s) responsible for writing the report, performing the research, or credited with the content of the report. The form of entry is the last name, first name, middle initial, and additional qualifiers separated by commas, e.g. Smith, Richard, J, Jr.

7. PERFORMING ORGANIZATION NAME(S) AND ADDRESS(ES). Self-explanatory.

8. PERFORMING ORGANIZATION REPORT NUMBER. Enter all unique alphanumeric report numbers assigned by the performing organization, e.g. BRL-1234; AFWL-TR-85-4017-Vol-21-PT-2.

9. SPONSORING/MONITORING AGENCY NAME(S) AND ADDRESS(ES). Enter the name and address of the organization(s) financially responsible for and monitoring the work.

10. SPONSOR/MONITOR'S ACRONYM(S). Enter, if available, e.g. BRL, ARDEC, NADC.

11. SPONSOR/MONITOR'S REPORT NUMBER(S). Enter report number as assigned by the sponsoring/ monitoring agency, if available, e.g. BRL-TR-829; -215.

12. DISTRIBUTION/AVAILABILITY STATEMENT. Use agency-mandated availability statements to indicate the public availability or distribution limitations of the report. If additional limitations/ restrictions or special markings are indicated, follow agency authorization procedures, e.g. RD/FRD, PROPIN, ITAR, etc. Include copyright information.

13. SUPPLEMENTARY NOTES. Enter information not included elsewhere such as: prepared in cooperation with; translation of; report supersedes; old edition number, etc.

14. ABSTRACT. A brief (approximately 200 words) factual summary of the most significant information.

15. SUBJECT TERMS. Key words or phrases identifying major concepts in the report.

16. SECURITY CLASSIFICATION. Enter security classification in accordance with security classification regulations, e.g. U, C, S, etc. If this form contains classified information, stamp classification level on the top and bottom of this page.

17. LIMITATION OF ABSTRACT. This block must be completed to assign a distribution limitation to the abstract. Enter UU (Unclassified Unlimited) or SAR (Same as Report). An entry in this block is necessary if the abstract is to be limited.